



Ceramide kinase regulates acute wound healing by suppressing 5-oxo-EETE biosynthesis and signaling via its receptor OXER1

Kenneth D. Maus¹, Daniel J. Stephenson¹, Anika N. Ali¹, Henry Patrick MacKnight¹, Huey-Jing Huang², Jordi Serrats², Minjung Kim¹, Robert F. Diegelmann³, and Charles E. Chalfant^{1,4,5,6,7,8,9,*}

¹Department of Cell Biology, Microbiology, and Molecular Biology, University of South Florida, Tampa, FL, USA;

²Neuroscience Drug Discovery Unit, Takeda California, San Diego, CA, USA; ³Department of Biochemistry and Molecular Biology, Virginia Commonwealth University-School of Medicine, Richmond, VA, USA; ⁴Cancer Biology and Evolution Program, The Moffitt Cancer Center, Tampa, FL, USA; ⁵Research Service, James A. Haley Veterans Hospital, Tampa, FL, USA; ⁶Division of Hematology & Oncology, Department of Medicine, and ⁷Department of Cell Biology, University of Virginia, Charlottesville, VA, USA; ⁸Program in Cancer Biology, University of Virginia Cancer Center, Charlottesville, VA, USA; ⁹Research Service, Hunter Holmes McGuire Veterans Administration Medical Center, Richmond, VA, USA

Abstract The sphingolipid, ceramide-1-phosphate (C1P), has been shown to promote the inflammatory phase and inhibit the proliferation and remodeling stages of wound repair via direct interaction with group IVA cytosolic phospholipase A₂, a regulator of eicosanoid biosynthesis that fine-tunes the behaviors of various cell types during wound healing. However, the anabolic enzyme responsible for the production of C1P that suppresses wound healing as well as bioactive eicosanoids and target receptors that drive enhanced wound remodeling have not been characterized. Herein, we determined that decreasing C1P activity via inhibitors or genetic ablation of the anabolic enzyme ceramide kinase (CERK) significantly enhanced wound healing phenotypes. Importantly, postwounding inhibition of CERK enhanced the closure rate of acute wounds, improved the quality of healing, and increased fibroblast migration via a “class switch” in the eicosanoid profile. This switch reduced pro-inflammatory prostaglandins (e.g., prostaglandin E₂) and increased levels of 5-hydroxyeicosatetraenoic acid and the downstream metabolite 5-oxo-eicosatetraenoic acid (5-oxo-EETE). Moreover, dermal fibroblasts from mice with genetically ablated CERK showed enhanced wound healing markers, while blockage of the murine 5-oxo-EETE receptor (oxoeicosanoid receptor 1) inhibited the enhanced migration phenotype of these cell models. Together, these studies reinforce the vital roles eicosanoids play in the wound healing process and demonstrate a novel role for CERK-derived C1P as a negative regulator of 5-oxo-EETE biosynthesis and the

activation of oxoeicosanoid receptor 1 in wound healing. **■** These findings provide foundational pre-clinical results for the use of CERK inhibitors to shift the balance from inflammation to resolution and increase the wound healing rate.

Supplementary key words arachidonic acid • inflammation • eicosanoids • lipidomics • group IVA phospholipases A₂ • 5-HETE • 5-oxo-EETE • ceramide-1-phosphate • ceramide kinase

The wound healing cascade is a dynamic process involving four distinct yet overlapping phases: hemostasis, inflammation, proliferation, and remodeling (1). Hemostasis is marked by vasoconstriction and the activation of clotting factors to reduce blood loss (2). Inflammation quickly follows to eliminate pathogens and external debris from the wound site (3, 4). Proliferation begins once foreign bodies have been removed by neutrophils and macrophages, allowing fibroblasts and keratinocytes to migrate into the wound site, ushering the transition from the inflammatory immune response and into the proliferative and angiogenetic phases (5). Lastly, new epithelial layers are formed, and collagen is cross-linked during the remodeling phase (6). Key factors in assessing wound maturation are the numbers and migration velocity of incoming fibroblasts, presence of fibroblast activation protein (FAP), and the deposition of collagen type I (7).

Our study focuses on the role of eicosanoids in wound healing, which are specialized lipid mediators with reported roles in mammalian wound response and the impairment of wound healing (8). For example, impaired wounds typically result from an imbalance between pro-inflammatory and anti-inflammatory eicosanoids such as prostaglandins and

*For correspondence: Charles E. Chalfant, cechalfant@virginia.edu or charles.chalfant@va.gov.

Current address for Jordi Serrats: Engrail Therapeutics, San Diego, CA, USA.

Current address for Huey-Jing Huang: ADARx Pharmaceuticals, San Diego, CA 92121, USA.



epoxyeicosatrienoic acids, respectively (9). Because of this, the blockade of cyclooxygenase-2-derived eicosanoids such as prostaglandin E₂ (PGE₂) is a long-used clinical technique to reduce inflammation (10). Localized excess of PGE₂ is linked to delayed wound healing and inhibition of fibroblast function (11), while various lipoxygenase (LOX)-derived eicosanoids have been tied to increased fibroblast chemotaxis and metabolic activity (12). Furthermore, fibroblast chemotaxis during wound healing is influenced by eicosanoids through unique receptors separate from peptide-mediated chemoattraction such as platelet-derived growth factor or epidermal growth factor (13). Overall, new technological advancements in small molecule analyses (e.g., lipidomics) (14) have identified a biochemical manifestation of impaired wound healing: the development of an imbalance between pro-inflammatory and anti-inflammatory eicosanoids independent of peptide mediators (1–13).

The synthesis of eicosanoids begins with the initial rate-limiting step, the generation of arachidonic acid (AA) via the activity of a phospholipase A₂ (PLA₂) (15). One of the major PLA₂s involved in this initial step is group IVA cytosolic PLA₂ (cPLA₂α), which our laboratory demonstrated is activated by direct binding to the sphingolipid, ceramide-1-phosphate (CIP) (16–21). For example, siRNA technology to downregulate ceramide kinase (CERK), the enzyme responsible for CIP formation, blocked cPLA₂α activation, AA release, and eicosanoid production in response to inflammatory cytokines, ATP, and calcium ionophore (16, 17). Previous findings from the Chalfant Laboratory demonstrated that the specific interaction site for CIP is localized to the calcium binding loop II of the C2 domain of cPLA₂α, specifically the cationic β-groove (19, 20). Mutagenesis of critical amino acids for CIP interaction within this site inhibited the ability of cPLA₂α to translocate in response to inflammatory agonists (21). These data suggest that CERK and its product, CIP, are required for the activation of cPLA₂α, and are thus major regulators of eicosanoid synthesis in cells. Our laboratory also discovered that CIP is temporally regulated, increasing in the inflammatory phase of human wound healing (22). Additional work by our laboratory has also recently shown that the CIP:cPLA₂α interaction negatively regulates the migration of dermal fibroblasts and 5-HETE production, and genetic ablation of this interaction enhanced acute wound healing in mice (23) (e.g. enhanced wound tensile strength, increased collagen I deposition, reduced collagen III deposition, and increased fibroblast wound infiltration).

In this study, our laboratory explored the source of CIP associated with the negative regulation of dermal fibroblast migration and wound healing. Specifically, we examined the hypothesis that inhibition of the formation of CIP via targeting the anabolic enzyme, CERK, either by genetic manipulations or by a new generation, small molecule inhibitors, will enhance the migration of

murine dermal fibroblasts in culture and into the acute wounds of mice as well as induce the downregulation of PGE₂ synthesis and upregulation of HETE production in murine dermal fibroblasts. Using a novel CERK inhibitor (SYR382141) in comparison to a conventional and established CERK inhibitor (N-[2-(Benzoylamino)-6-benzothiazoly]tricyclo[3.3.1.1.3,7]decane-1-carboxamide [NVP-231]) and genetically engineered mouse models, either an ablated CIP interaction site (cPLA₂α-KI) or CERK ablated (CERK-knockout [CERK-KO]), we show that inhibition/ablation of CERK confers a distinct lipid “fingerprint” consistent with dermal fibroblasts that confers more rapid cell migration and accelerates the transition from inflammation to proliferation. In expanded mechanistic studies, a distinct role for the 5-HETE metabolite, 5-oxo-eicosatetraenoic acid (5-oxo-ETE), was shown to facilitate enhanced fibroblast migration through a murine G protein-coupled oxoeicosanoid receptor (OXER1). Lastly, we found that the inhibition of CERK, postwounding, conferred enhanced wound healing and maturation providing a preclinical foundation to explore human clinical applications. Overall, these studies show that CERK-derived CIP inhibits the proliferation/remodeling stages of wound healing showing the therapeutic relevance of CERK inhibitors in this paradigm.

MATERIALS AND METHODS

SYR382141 compound

A request to access the CERK inhibitor SYR382141 should be made directly to the Neuroscience Drug Discovery Unit, Takeda California, San Diego, CA.

PCR-based identification of WT, cPLA₂α-KI, and CERK-KO

Genotyping of WT, cPLA₂α-KI, and CERK-KO mice was performed by first collecting genomic DNA using an AccuStart II genotyping kit followed by PCR as previously described (24, 25) using the following primers: KI: PLA2 58534–58556, 5′-TGAGGGTCGTGCTGTAGAGTTAG-3′; PLA2 58780–58757, 5′-TGCCAGATGTGAACTTACTTCCAG-3′; KO: cre primers (5′-ATATCTCACGTAAGTACGGTGGG-3′) (P1), and (5′-CCTGTTTCACTATCCAGGTTACGG-3′) (P2) (supplemental Fig. S1). Fifty nanograms of genomic DNA was used for each reaction along with the following primer concentrations, KI: 0.2 μmol/L PLA2 58534–58556 (P1), 0.2 μmol/L PLA2 58780–58757 (P2), and CERK-KO: 0.2 μmol/L P1 and 0.2 μmol/L P2. The following reaction cycles were repeated 33 times, 94°C for 1 min, 59°C for 1 min, and 72°C for 2 min. Reaction products expected are as follows: cPLA₂α-WT: 237 bp, cPLA₂α-KI: 412 bp, CERK-WT: 207, and CERK-KO: 480 bp and were examined using a 2% agarose gel.

RT-qPCR analysis of mRNA expression

RNA from WT and CERK-KO primary dermal fibroblasts was converted to cDNA and used for quantitative PCR analysis using primers specific to the mouse *Cerk* gene (Thermo)

and mouse actin control (Thermo). Methods is as previously described (26–28) (supplemental Fig. S1).

Acute wound healing in mice

The acute wound closure rate was examined in mice as recently reported by us (23). Specifically, a 5 mm biopsy punch was performed on the dorsum of each mouse. Silicone stints were then placed around the wound, and a combination of sutures and glue was used to hold said stints in place. Wounds were dressed using Tegaderm (3M Medical) and imaged over the course of 10 days. Wound images were analyzed using the Fiji image J bundle. Wounds were tracked as percent of initial wound size over 10 days with or without CERK inhibition via small molecule inhibitor SYR382141 or genetic ablation (*CERK*-KO mouse). Treatment groups ($n = 5$ mice/group) are as follows: untreated, carboxymethyl cellulose sham control (1% carboxymethyl cellulose), 60 mg/kg SYR382141. The sham and SYR382141 groups received an oral gavage twice a day for nine days starting on day 1. Statistical analyses included two-way ANOVA with Tukey post hoc. A significant difference was determined by a $P < 0.05$. At the end of 10 days, tissues, blood, and wounds were harvested.

Histology

Six millimeter samples of wound tissue were excised after 10 days; wounds were prepared for histological evaluation using the following procedure, as previously described (29). Excised wounds were fixed by placing them in 4% paraformaldehyde for 24 h; following fixation, the wound was placed in a cassette that allowed for the dehydration of the tissue, followed by clearing of the tissue using xylene (Fisher brand), and finally imbedding the tissue in paraffin wax. Sections (5 μ m) of the paraffin block were placed on clear glass slides for further treatment and staining. Staining with Masson's trichrome and hematoxylin and eosin was performed. Rabbit polyclonal anti-FAP, alpha antibody (Abcam; ab53066; 1:100) and rabbit polyclonal anti-type I collagen (Abcam ab34710; 1:200) were used in immunohistochemical staining followed by anti-rabbit secondary antibody from Vectastain Elite kit (VectorLabs PK-6100) and avidin-biotin complex enhancement. All sections were visualized with Vector NovaRED Chromogen kit (VectorLabs SK-4800) and counterstained with hematoxylin. Slides were viewed on Keyence BZ-X710 microscope and analyzed using the Fiji image J bundle for watershed cell counting or high-contrast stained area calculation, where appropriate.

Isolation of mouse dermal fibroblast

Primary mouse dermal fibroblasts (pDFs) were isolated from 10-week-old WT, *CERK*-KO, and *cPLA α* -KI BALB/c males as previously described (30). Once harvested, cells were cultured using high glucose DMEM (Gibco) supplemented with 20% FBS (Gibco) and 2% penicillin/streptomycin (Bio Whittaker) at standard incubation conditions. Cells were not used after passage 5.

Scratch-induced mechanical trauma of fibroblasts

pDFs obtained from WT, *CERK*-KO, and *cPLA α* -KI mice were plated at a density of 2×10^6 on 100 mm tissue culture plates in high glucose DMEM supplemented with 10% FBS (Gibco) and 2% penicillin/streptomycin (Bio Whittaker) and

left overnight to adhere at standard incubation conditions. Following the overnight incubation, cells were rested in 2% FBS (Gibco), 2% penicillin/streptomycin (Bio Whittaker), and high glucose DMEM (Gibco) for 2 h. After the 2 h resting period, mechanical trauma was induced on the monolayer by performing scratches across the diameter of the plate in an asterisk pattern using four 20 μ l pipette tips on a multichannel micropipette. Media were taken for lipidomic analysis at multiple time points (0 h and 2 h).

Exogenous addition of CERK inhibitors to human umbilical vein endothelial cells and human leukemia 60 cells

Human umbilical vein endothelial cells (HUVECs) were plated at a density of 2×10^5 cells in a 6-well plate containing endothelial cell growth medium-2 with BulletKit supplements (Lonza; catalog no.: CC-3162) and allowed to rest overnight. Human leukemia (HL) 60 cells were plated at a density of 1×10^6 cells in 100 mm tissue culture plates containing Iscove's Modified Dulbecco's Medium (ThermoFisher; catalog no.: 12200036) with 10% FBS (Gibco). After the resting period, media were aspirated and replaced with new growth media containing the addition of inhibitors (100 nM SYR382141, 300 nM NVP-231, or 0.001% DMSO control) and allowed to rest for another 24 h before media and cell lysate collection for lipid analysis, as previously described (31).

Analysis of eicosanoids by ultra performance liquid chromatography ESI-MS/MS

Eicosanoids were separated using a Shimadzu Nexera X2 LC-30AD coupled to a SIL-30AC auto injector, coupled to a DGU-20A5R degassing unit in the following way as previously described (32). A 14 min reversed phase LC method utilizing an Ascentis Express C18 column (150 mm \times 2.1 mm, 2.7 μ m) was used to separate the eicosanoids at a 0.5 ml/min flow rate at 40°C as previously described by us (33–35). The column was equilibrated with 100% solvent A [acetonitrile:water:formic acid (20:80:0.02, v/v/v)] for 5 min and then 10 μ l of sample was injected. Hundred percent solvent A was used for the first two minutes of elution. Solvent B [acetonitrile:isopropanol:formic acid (20:80:0.02, v/v/v)] was increased in a linear gradient to 25% solvent B at 3 min, to 30% at 6 min, to 55% at 6.1 min, to 70% at 10 min, and to 100% at 10.10 min. Hundred percent solvent B was held constant until 13.0 min, where it was decreased to 0% solvent B and 100% solvent A from 13.0 min to 13.1 min. From 13.1 min to 14.0 min, solvent A was held constant at 100%. Eicosanoids were analyzed via MS using an AB Sciex Triple Quad 5500 mass spectrometer as previously described (36). Q1 and Q3 were set to detect distinctive precursor and product ion pairs. Ions were fragmented in Q2 using N2 gas for collisionally induced dissociation. Analysis used multiple reaction monitoring in negative ion mode. Eicosanoids were monitored using precursor \rightarrow product MRM pairs. The mass spectrometer parameters were as previously described (37, 38): curtain gas: 20; collisionally activated dissociation: medium; ion spray voltage: -4500 v; temperature: 300°C; gas 1: 40; gas 2: 60; declustering potential, collision energy, and cell exit potential vary per transition.

Migration analysis of fibroblasts

Cells were seeded into 24-well tissue culture plates at a density of 7.5×10^4 and allowed to grow to confluence. Once a confluent monolayer was achieved, cells were placed in 2%

FBS (Gibco)/2% penicillin/streptomycin (Bio Whittaker) high glucose DMEM media and allowed to rest for 2 h. After the 2 h resting period, mechanical trauma was induced on the monolayer by performing a single scratch across the diameter of each well using a 20 μ l pipette tip. Cells were observed using a live cell incubation chamber maintained at 37°C in a 95% air/5% CO₂ atmosphere mounted on a Keyence BZ-X710 microscope, which took images every 3 min for 24 h. Migration velocity was calculated using the Keyence VW-9000 motion analysis software as previously described (23).

Exogenous addition of eicosanoids/inhibitors on dermal fibroblasts

pDFs were seeded into 24-well tissue culture plates at a density of 7.5×10^4 and allowed to grow to confluence. Once a confluent monolayer was achieved, cells were placed in 2% FBS (Gibco) high glucose DMEM media (Gibco) containing the addition of various eicosanoids and/or inhibitors at the following concentrations (1.0 nM 5-HETE, 1.0 nM 5-oxo-EETE, 7.5 nM MK886, 10 μ M Gue1654, 100 nM SYR382141, 100 nM NVP-231) and allowed to rest. After the 2 h resting period, mechanical trauma was applied as mentioned previously, and the media were exchanged with fresh 2% FBS (Gibco) and high glucose DMEM media (Gibco) containing the addition of various eicosanoids at the aforementioned concentrations.

Statistical analysis

Graphing and statistics were performed using Prism GraphPad (Prism Software, San Diego, CA). Data were analyzed via ANOVA followed by Tukey's post hoc test or Dunnett's multiple comparisons test where applicable. All data were reported as mean \pm standard deviation (SD); $P < 0.05$ was considered statistically significant.

Ethical considerations

All mouse studies were undertaken under the supervision and approval of the USF IACUC (Protocol# IS00004094 and IS00004110) following standards set by the Federal and State government. USF is fully accredited by AAALAC International as program #000434.

RESULTS

SYR382141 inhibits CIP production in multiple cell types

Previously, our laboratory reported that the interaction of CIP and group IVA PLA₂ was a negative regulator of acute wound healing and the migration of dermal fibroblasts, but the source of CIP was not known. To examine the source of CIP for these phenotypes, we obtained a new generation inhibitor of one known source of mammalian CIP, CERK, which was developed by Takeda Corporation and designated SYR382141 and evaluated via previously described analyses (39–45). This compound inhibited CERK activity in vitro with an IC₅₀ of 5 nM for human CERK and 9 nM for mouse CERK. SYR382141 did not significantly affect the activity of closely related kinases such as

sphingosine kinase 1 and 2 (>100 μ M, [supplemental Table S1](#)) as well as kinases in a global kinase panel (1 μ M; [supplemental Table S1](#)). SYR382141 also demonstrated an IC₅₀ of >30 μ M to induce cytotoxicity in tissue culture ([supplemental Table S1](#)). To evaluate the ability of SYR382141 to inhibit CERK-derived CIP production in cells, pDFs and HUVECs were treated with SYR382141 or the positive control, the CERK inhibitor NVP-231, and analyzed via ultra performance liquid chromatography coupled with electrospray ionization tandem mass spectrometry (22, 36) ([Fig. 1](#)). The levels of detectable CIP species, D-e-C_{16:0} CIP (C16:0), D-e-C_{14:0} CIP (C14:0), D-e-C_{24:0} CIP (C24:0), and D-e-C_{24:1} CIP (C24:1) were significantly reduced by SYR382141 in pDFs to an equivalent or greater extent as NVP-231 (17) using nanomolar concentrations ([Fig. 1A](#)). Similar results were observed in HUVECs ([Fig. 1B](#)). Pharmacokinetically, SYR382141 treatment of mice demonstrated significant plasma concentrations over 4 h, which would allow for initial preclinical studies on the effectiveness of inhibiting CERK in modulation of the in vivo phenotype, acute wound healing ([supplemental Table S2](#)). These data demonstrate that nanomolar concentrations of SYR382141 significantly block the production of CERK-derived CIP in cells analogous to an established inhibitor of the enzyme, but importantly, SYR382141 can be utilized to inhibit CERK in mice.

CERK inhibition and genetic ablation improves wound closure rate and healing quality in vivo

To determine whether CERK inhibitors could recapitulate the enhanced wound healing observed in a genetically engineered mouse model where the CIP binding site in cPLA₂ α was ablated (cPLA₂ α KI mice; KI) (23), WT mice were subjected to an acute excisional wound. One day post-wounding, WT mice were treated twice daily, orally with the new generation CERK inhibitor, SYR382141, versus the control (sham) and untreated mice. The dose of SYR382141 utilized showed significant levels of the drug in mouse tissues (e.g., kidney) ([supplemental Table S3](#)), and importantly, a significant increase in the rate of wound closure was observed after 10 days ([Fig. 2](#)). CERK inhibition dramatically increased the presence of FAP and subsequent pDFs in the acute wounds at 10 days ([Fig. 3](#)). Furthermore, both the Masson's trichrome stain and immunohistochemistry analysis for type I collagen staining indicate enhanced collagen type I deposition. To confirm the specificity of the effect of SYR382141 via CERK inhibition, a novel CERK-KO mouse was examined in the same context, but in the absence of SYR382141 treatment ([supplemental Fig. S1](#)), which also showed a significant increase in the rate of wound closure at days 6–10 ([Fig. 2](#)) as well as enhanced pDFs (FAP staining) and collagen type I in the wounds ([Fig. 3](#)). These data indicate that CIP derived from

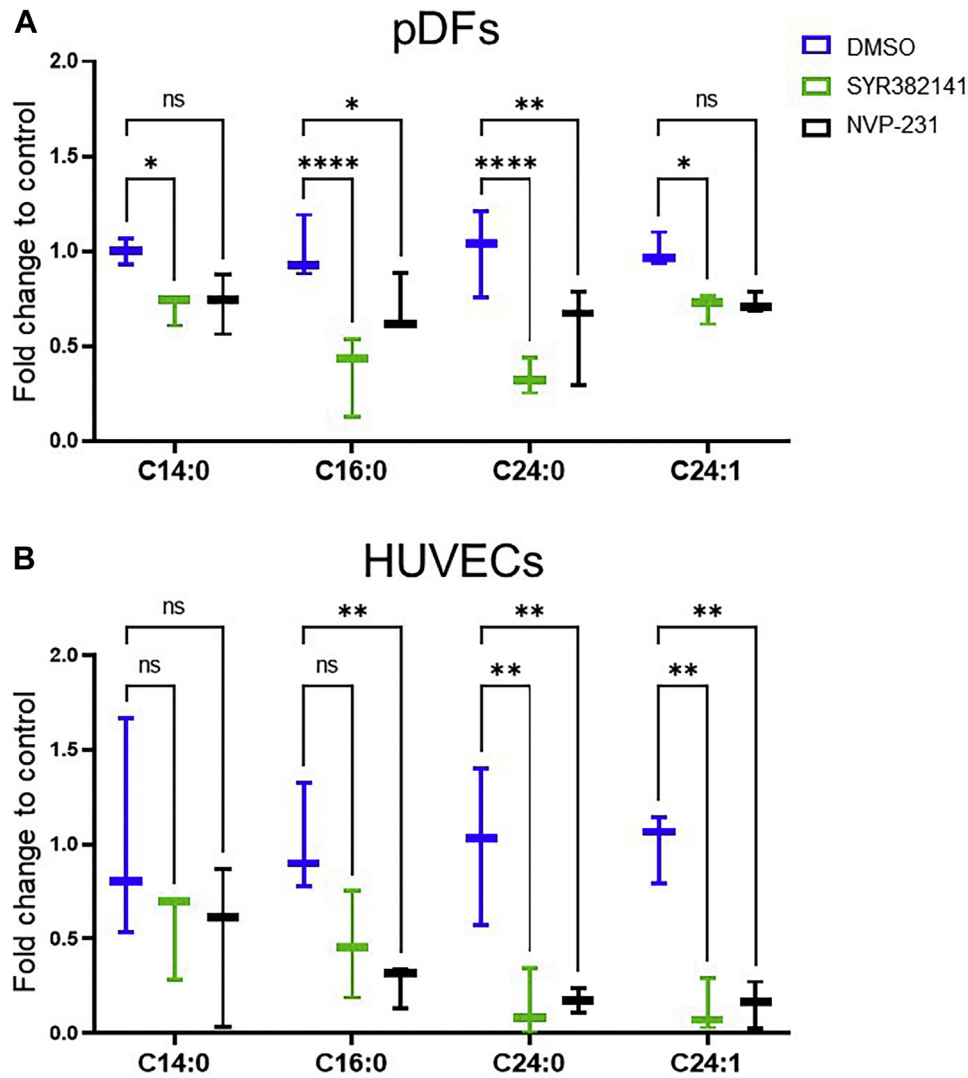


Fig. 1. SYR382141 decreases ceramide-1-phosphate levels in cells. A: WT pDFs pretreated with SYR382141 (100 nM), NVP-231 (100 nM), or DMSO (0.01%) for 30 min received mechanical trauma via asterisk pattern scratch across the plate. Cells were collected 2 h post-injury and analyzed for CIP levels via UPLC ESI-MS/MS. Values expressed as fold change to DMSO controls (* $P < 0.05$, ** $P < 0.01$, *** $P < 0.0001$; $n = 3$, pDFs collected from three different mice; two-way ANOVA with Dunnett's multiple comparisons test). B: HUVECs were treated with SYR382141 (100 nM), NVP-231 (300 nM), or DMSO (0.01%) for 24 h. Cells were collected and analyzed for CIP levels via UPLC ESI-MS/MS. Values expressed as fold change to DMSO controls. (* $P < 0.05$, ** $P < 0.01$, *** $P < 0.001$; $n = 3$; one-way ANOVA with Tukey post-hoc test).

CERK acts as a negative regulator of fibroblast migration into the wound environment, and inhibition or genetic ablation of *CERK* significantly enhances acute wound healing and maturation. Furthermore, inhibition of *CERK* is beneficial to acute wound healing in a post-wounding manner.

CERK inhibition enhances dermal fibroblast migration

To examine specific mechanisms that may contribute to an improved wound healing rate, pDFs were cultured *ex vivo* from WT and homozygous *CERK*-KO (*CERK*^{-/-}; *CERK*-KO) mice along with a positive control, pDFs cultured from homozygous *cPLA₂* knockin mice with the CIP interaction site ablated (*cPLA₂* KI) (23). As previously reported (23),

cPLA₂-KI fibroblasts migrated more rapidly than WT (Fig. 4A, B). The same increase in migration velocity was also observed for WT pDFs with inhibition of *CERK* using SYR382141 or the *CERK* inhibitor, NVP-231, versus sham controls (Fig. 4A, B). Additionally, pDFs from mice with *CERK* genetically ablated (*CERK*-KO), which produce a similar reduction in CIP to SYR382141-treated pDFs (Fig. 4C), also showed a similar migration velocity profile to that of SYR382141-treated WT and *cPLA₂*-KI fibroblasts (Fig. 4A, B). Also of note, addition of SYR382141 or NVP-231 was unable to further enhance the migration velocities of *cPLA₂*-KI or *CERK*-KO pDFs (Fig. 4B). Lipidomic analysis of SYR382141-treated WT pDFs as well as *CERK* KO pDFs after mechanical trauma showed significant increases in multiple LOX-derived

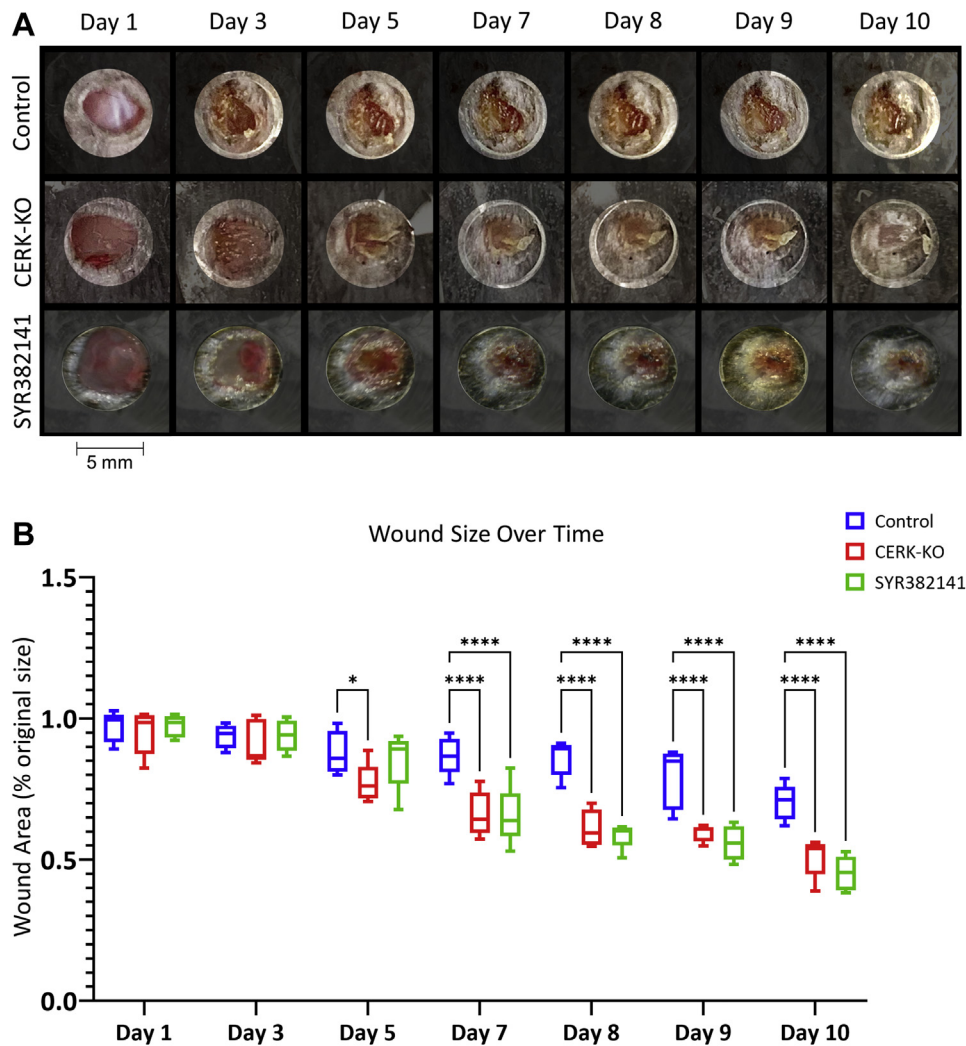


Fig. 2. Inhibition of ceramide kinase increases the closure rate of acute wounds in mice. **A:** Wound closure rate of 5 mm biopsy wound on dorsum of *CERK-KO* or WT mice treated with carboxymethyl cellulose (CMC) control (1% CMC) or SYR382141 (60 mg/kg), orally twice daily beginning 1 day post-injury (1 wound per mouse repeated on two separate occasions). **B:** Graph depicting acute wound closure rate quantified as percent of initial wound size over 10 days. Two-way ANOVA with Dunnett's multiple comparisons test, * $P < 0.05$, **** $P < 0.0001$; $n = 5$ wounds per genotype, 1 per mouse.

HETE species (e.g., 5-HETE, 12-HETE, 15-HETE), and the more bioactive metabolite of 5-HETE, 5-oxo-EETE, and the pro-inflammatory prostaglandin, PGE₂, trended downward (Fig. 4D). Changes in 5-HETE and 5-oxo-EETE production became evident as early as 60 min postinjury, but no changes in the levels of the CERK substrate, ceramide, were observed (supplemental Fig. S3A, B). Similar eicosanoid profiles were observed in HUVECs and HL-60 cells treated with NVP-231 (supplemental Fig. S2). Lipidomic analysis of wound tissue from healed wounds in SYR382141-treated mice displayed significant increases in 5-HETE and 5-oxo-EETE but did not show the reduced PGE₂ levels observed in pDFs treated with CERK inhibitors (Fig. 5). These data demonstrate that CIP derived from the anabolic enzyme, CERK, is a negative regulator of 5-oxo-EETE biosynthesis and pDF migration via direct association with cPLA₂α.

Enhanced dermal fibroblast migration requires 5-HETE/5-oxo-EETE signaling via an OXER1-like receptor

To determine whether the 5-HETE/5-oxo-EETE derived via the 5-LOX/5-lipoxygenase-activating protein pathway drives pDF migration in a paracrine/autocrine manner, we employed the 5-lipoxygenase-activating protein inhibitor MK886 to prevent 5-HETE/5-oxo-EETE production and Guel654, a non-Gα_i-biased antagonist of human OXER1, which blocks 5-oxo-EETE-triggered functional events (46). MK886 and Guel654 effectively reduced cPLA₂α KI and *CERK-KO* pDF migration velocity to that of WT pDFs and blocked SYR382141 effects on the WT pDFs (Fig. 6). A combination of MK886 and Guel654 did not act additively or synergistically to block the effect of the genetic ablation of the CIP/cPLA₂α interaction or CERK inhibition. These data demonstrate that 5-HETE/5-oxo-EETE drive

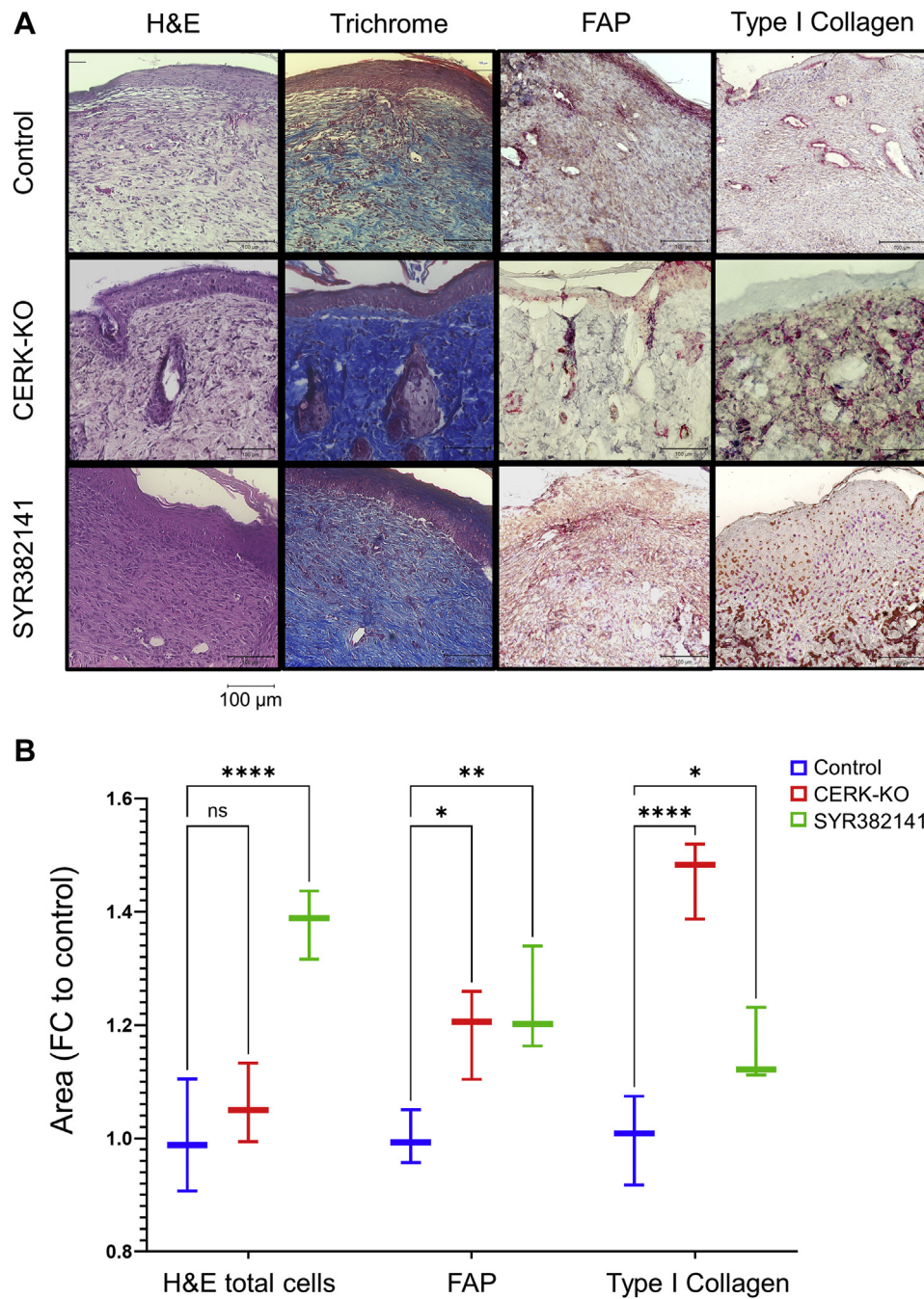


Fig. 3. Inhibition and genetic ablation of ceramide kinase improve wound quality. **A:** Wound tissue harvested 10 days post-injury from WT control (1% CMC), *CERK*-KO, and SYR382141-treated (60 mg/kg) WT mice under H&E (cell infiltration), Masson's Trichrome (collagen deposition), FAP (fibroblast activation protein), and type I collagen staining. **B:** Graph depicting quantification of infiltrating cells, FAP area, and type I collagen area, analyzed via ImageJ cell counter and Fiji ImageJ bundle area tool, contrast enhanced (* $P < 0.05$, ** $P < 0.01$, *** $P < 0.001$, **** $P < 0.0001$; $n = 3$ samples per treatment group, 1 wound per mouse; two-way ANOVA with Dunnett's multiple comparisons test).

the enhanced migration in *cPLA₂* KI and SYR382141-treated or *CERK*-ablated pDFs via autocrine/paracrine signaling through a murine G-protein-coupled OXER1.

DISCUSSION

In this study, we characterized both a new *CERK*-KO mouse and a new small molecule inhibitor of CERK in the context of an enhanced wound healing phenotype.

Specifically, we showed that inhibition of CERK-derived CIP could recapitulate the finding that genetic ablation of the CIP/*cPLA₂* interaction site enhances acute wound healing through increased dermal fibroblast migration and accelerated type I collagen deposition characteristic of nonfibrotic healed wounds (22). In this regard, *CERK* ablation or inhibition with this novel compound did recapitulate enhanced acute wound healing, and importantly, this effect occurred

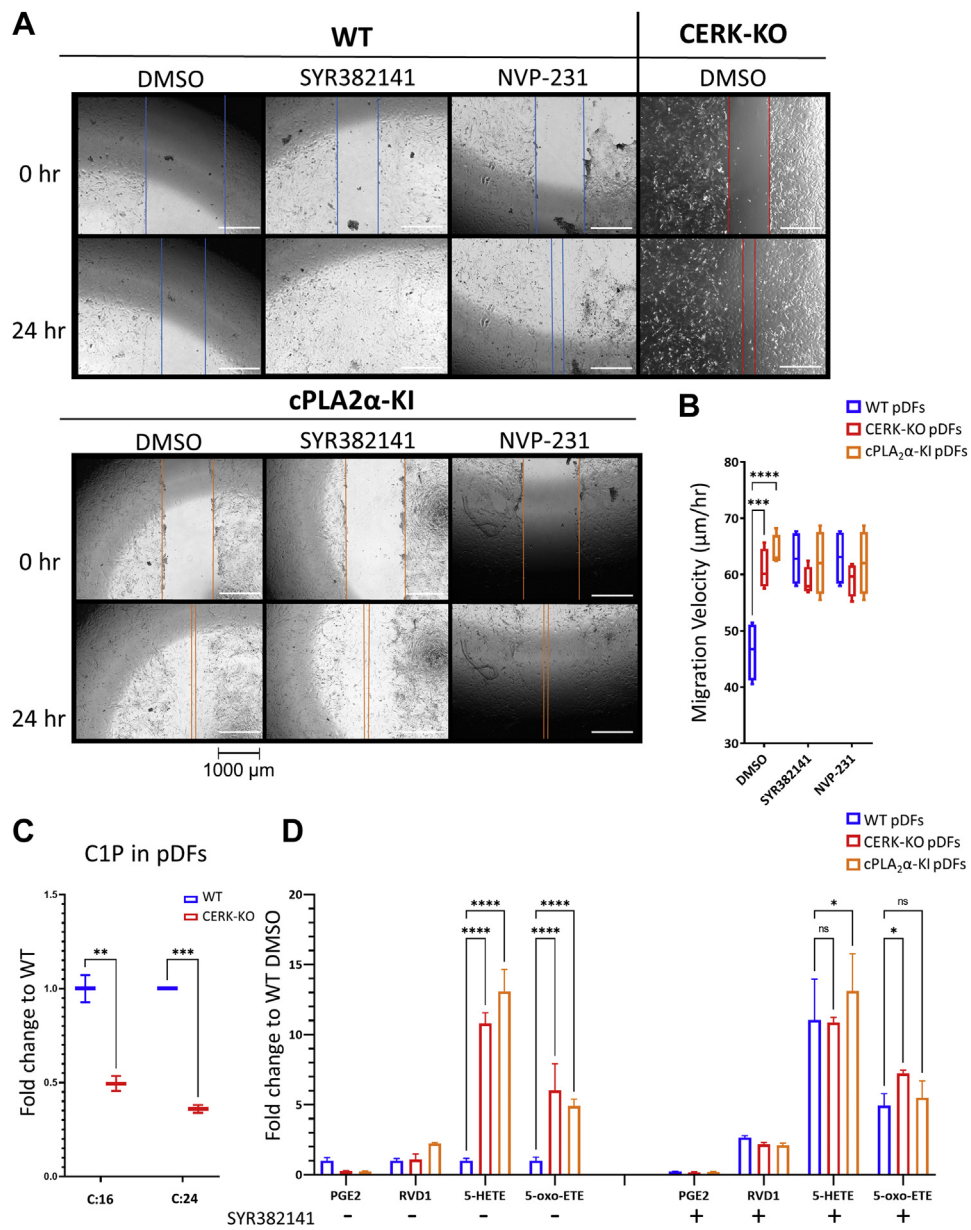


Fig. 4. Inhibition or genetic ablation of ceramide kinase enhances the migration of dermal fibroblasts and HETE biosynthesis. A: pDFs from WT, *CERK*-KO, and *cPLA₂α*-KI mice treated with DMSO (0.001%), SYR382141 (100 nM) or NVP-231 (100 nM). Still images from time points 0- and 24-h. Brightness enhanced; lines added for emphasis. Cells were observed using a live cell incubation chamber mounted on a Keyence BZ-X710 microscope which took images every 3 min for 24 h (n = 4; pDFs taken from two separate animals per genotype). B: Graph depicting migration velocities of pDFs treated with CERK inhibitors SYR382141 (100 nM) or NVP-231 (100 nM), calculated using the Keyence VW-9000 motion analysis software (Dunnett's multiple comparisons test; n = 4; pDFs taken from two separate animals per genotype). C: C1P (C:16 (C16:0) and C:24 (C24:0)) production in wound tissue from *CERK*-KO mice compared to WT (n = 4 per genotype; one wound per mouse). D: Eicosanoids from WT, *CERK*-KO, and *cPLA₂α*-KI pDFs pretreated with SYR382141 or DMSO control collected 2 h after mechanical injury (two-way ANOVA with Dunnett's multiple comparisons test; **P* < 0.05, ***P* < 0.01, ****P* < 0.001, *****P* < 0.0001; n = 3, pDFs taken from three separate mice per genotype).

post-wounding and thus sets the foundational preclinical studies to move forward for future clinical efficacy studies. Furthermore, this study determines the source of CIP activating *cPLA₂α* signaling in suppressing dermal fibroblast migration and wound maturation as CERK versus another means of CIP biosynthesis like the reported mammalian SIP acylase activity (47).

This study also expanded the mechanistic knowledge as to how the association of CERK-derived CIP with

cPLA₂α drives enhanced wound healing, wound maturation, and pDF migration/collagen deposition. More specifically, this study demonstrated that CERK-derived CIP negatively regulates 5-HETE biosynthesis with 5-HETE, but also showed that 5-HETE was metabolized to 5-oxo-EETE, which is 100-fold more biologically active. This 5-HETE metabolite was found to act in an autocrine/paracrine manner by activating a murine OXER1 receptor to enhance pDF migration

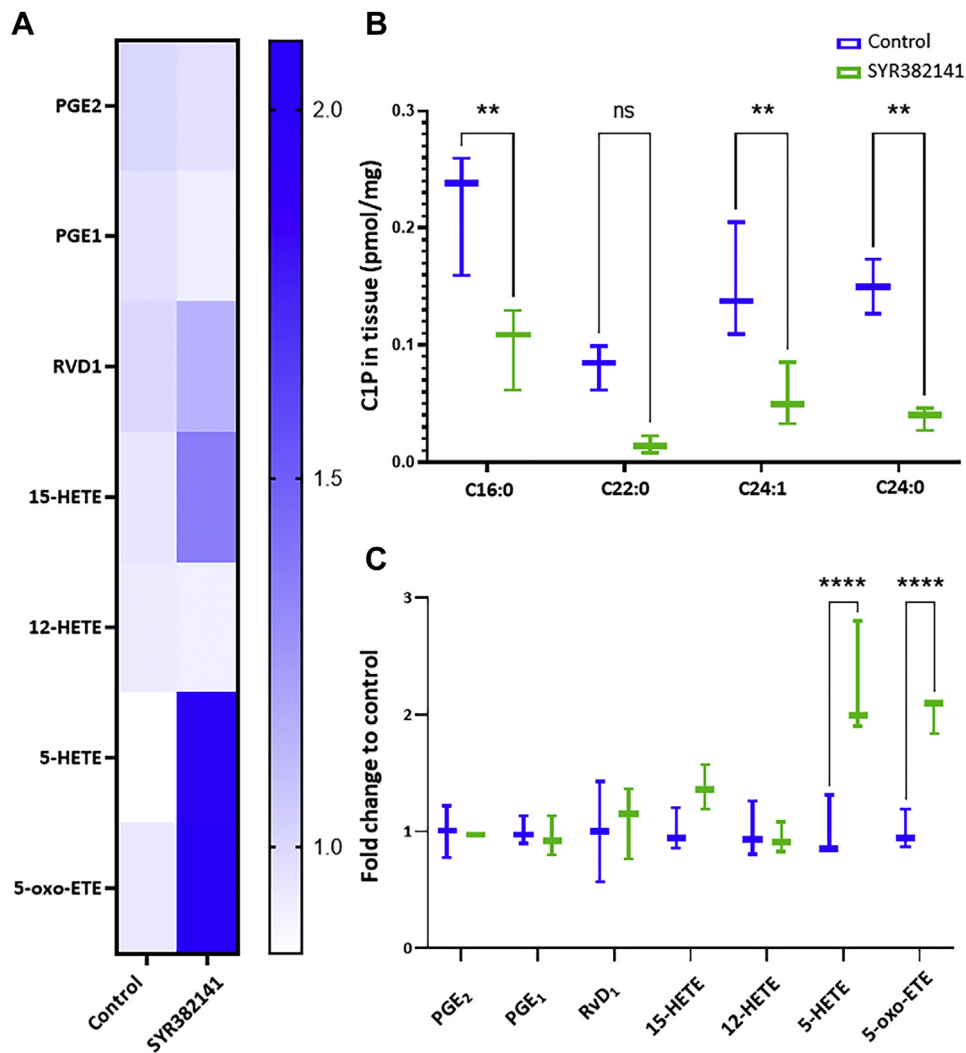


Fig. 5. Inhibition of ceramide kinase enhances 5-HETE and 5-oxo-EETE biosynthesis in acute wounds. A: Heatmap representation of eicosanoid profile of wound tissue harvested 10 days post-injury from WT mice treated with SYR382141 (60 mg/kg) or control (1% CMC) (n = 3 per treatment group; 1 wound sample per mouse). B: Graphical comparison of CIP profile of wound tissue harvested 10 days post-injury (n = 3 per treatment; 1 wound sample per mouse; two-way ANOVA with Šidák's multiple comparisons test). C: Graph depicting eicosanoid profile of wound tissue harvested 10 days post-injury, (* $P < 0.05$, ** $P < 0.01$, *** $P < 0.001$, **** $P < 0.0001$; n = 3 per treatment group; 1 wound sample per mouse; two-way ANOVA with Šidák's multiple comparisons test).

(Fig. 7). The murine OXER1 receptor has yet to be defined unlike the homolog to the human OXER1 receptor. Regardless, the effectiveness of the OXER1 antagonist, Guel654, which blocks both 5-HETE and 5-oxo-EETE effects on pDF migration, shows the existence of an undefined homolog of the human OXER1. A recent report by Lai *et al.* (48) also demonstrates that the uncharacterized murine OXER1 receptor does exist in mice due to successful treatment with Guel654 affecting coronary artery ligation-induced ischemic myocardial injury. Homology analysis shows that the mouse hydroxycarboxylic acid receptor 2 (HCAR2), which has been proposed to mediate 5-oxo-EETE responses in mice (49) and shares approximately 42% homology with human OXER1, is highly expressed in adipose tissue and macrophages and is expressed 3- to 5-fold higher when exposed to inflammatory mediators (e.g., lipopolysaccharide, tumor necrosis factor α ,

interleukin 1) (50). However, future studies need to confirm this murine receptor as the target for Guel654 in mice to block 5-HETE and 5-oxo-EETE biological responses. Preliminary studies from our group utilizing compounds reported to nonspecifically downregulate murine HCAR2 in pDFs show similar migration inhibition effects as Guel654 supporting the hypothesis that HCAR2 is the 5-oxo-EETE receptor in mice. Overall, this study can conclude that an OXER1 G-protein-coupled receptor exists in mice, which is required for 5-HETE and 5-oxo-EETE to enhance pDF migration, but this study cannot confirm the exact receptor homolog to human OXER1 at this time.

Notably, both the loss of CIP/cPLA $_2\alpha$ interaction and the inhibition of CERK resulted in dramatic decrease of inflammatory prostaglandins concomitant with 5-HETE increase. Indeed, CIP reportedly increases during the inflammatory stage of wound healing in

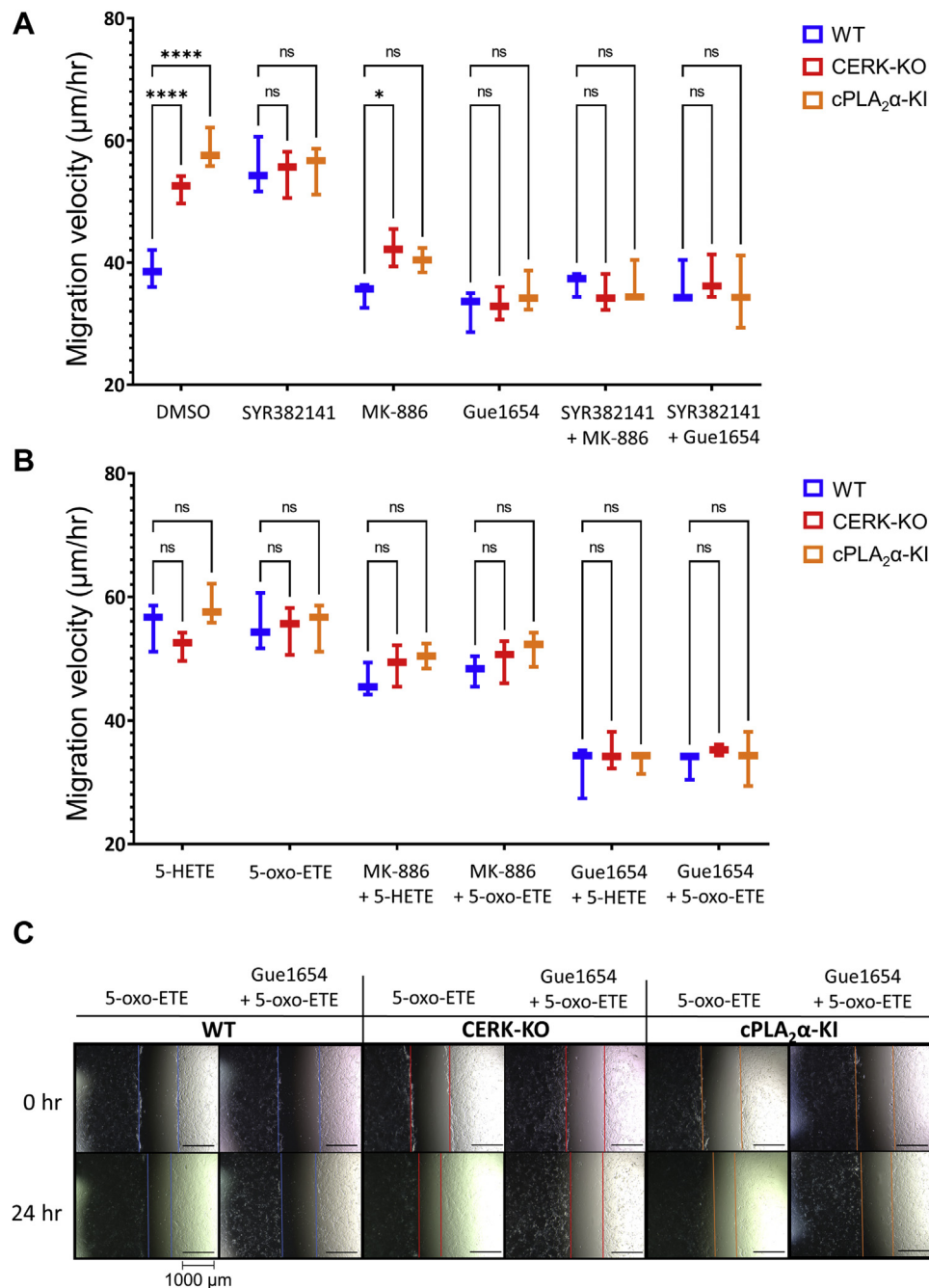


Fig. 6. A: Graph depicting pDF migration velocity of WT, *CERK-KO*, and *cPLA₂α-KI* pDFs treated with combinations of FLAP inhibitor MK886 (7.5 nM), OXER1 antagonist Gue1654 (10 µM), ceramide kinase inhibitor SYR382141 (100 nM). All values compared to WT DMSO control (n = 3 per treatment; pDFs taken from three separate mice per genotype; two-way ANOVA with Dunnett's multiple comparisons test; **P* < 0.05, ***P* < 0.01, ****P* < 0.001, *****P* < 0.0001). B: Graph depicting pDF migration velocity of WT, *CERK-KO*, and *cPLA₂α-KI* pDFs treated with combinations of 5-HETE (100 nM), and 5-oxo-ETE (1 nM) treatments in combination with MK886 (7.5 nM) and Gue1654 (10 µM). All values compared to panel (A) WT DMSO control (n = 3 per treatment; pDFs taken from three separate mice per genotype; two-way ANOVA with Dunnett's multiple comparisons test; **P* < 0.05, ***P* < 0.01, ****P* < 0.001, *****P* < 0.0001). C: Representative microscope images of 5-oxo-ETE rescue and Gue1654 suppression of pDF migration from data graphed in panels A and B. Contrast enhanced, lines added for emphasis.

human subjects but then decreases during the proliferation and remodeling stages (51). These findings, when coupled with CIP being a negative regulator of proliferation and wound maturation (23), suggest that CIP is a pro-inflammatory mediator modulating the inflammatory stage and an essential “stop-gap” in the

subsequent activation of the proliferation stage. Thus, blocking CIP production or CIP interaction with *cPLA₂α* proves to be beneficial for condensing the inflammatory phase and inducing the proliferation/remodeling phases earlier by enhancing fibroblast activity. Interestingly, *CERK* inhibitors also increased

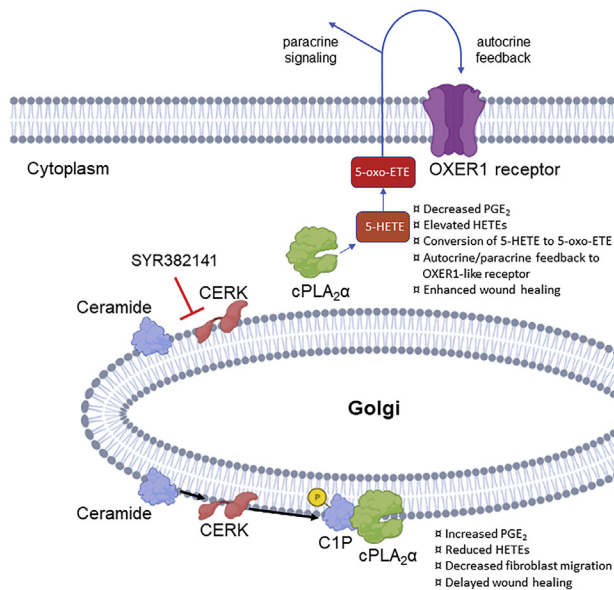


Fig. 7. Inhibition of CERK-induced CIP elevates 5-HETE and its conversion to 5-oxo-EETE and subsequent action on OXER1-like receptor resulting in increased fibroblast activity and expedited wound healing. The presence of CERK results in elevated CIP, leading to an eicosanoid shift from HETEs to PGE₂ resulting in delayed wound healing via reduced fibroblast migration.

other proresolution 15-LOX-derived eicosanoids such as 15-HETE and RVD₁ in various cell types. These data further suggest that CIP may regulate additional PLA₂ isoforms, which regulate the production of these specific eicosanoids. One possibility could be cPLA₂ β , which has not been well characterized and contains a C2-domain analogous to cPLA₂ α (52, 53).

One conundrum from our study is the observation that inhibition of CIP improves pDF migration. Although congruent with our previous finding in mouse embryonic fibroblasts with *CERK* ablated, other laboratories have reported that CIP treatment induces cellular migration in macrophages (54) and pancreatic cells (55). We hypothesize that these differences may be due to the cellular localization of CIP. For instance, exogenous CIP treatment using a vesicle-based delivery mainly increases the CIP content of the plasma membrane (PM) in various cell types (56) with rapid metabolism to ceramide observed (36). This PM pool of CIP may encourage migration via association with factors such as annexins (32). Additionally, the reported opposing functions of CIP on cell migration may be due to cell type-specific variances as in our studies. Indeed, our studies utilize fibroblasts, whereas other reports show that CIP enhances macrophage migration (54). Inhibition of CIP may reduce macrophage-induced inflammation in the wound, which is a plausible mechanism to accelerate dermal wound healing. Our current study argues against a cell type-specific variance as we show that both HUVECs and HL-60 cells increase 5-HETE and 5-oxo-EETE in response to

CERK inhibition, and thus, any context variations are likely due to differences in OXER1 activation in specific cell types.


Metabolism to other sphingolipids that drive cellular migration may also be a plausible explanation for the differential reports on CIP in cell migration (e.g., catabolism to sphingosine-1-phosphate) (57). Furthermore, an additional anabolic pathway for CIP generation does exist in mammalian cells, which may involve a sphingosine-1-phosphate-acylase (47) at the PM. CERK-derived CIP is more recognized as a Golgi form of CIP (58) and associated with cPLA₂ α activation and eicosanoid biosynthesis. The form of CIP may inhibit migration due to association with cPLA₂ α localized to this organelle and modulation of specific eicosanoids (e.g., PGE₂) (58). Additionally, transport of CIP to the PM by CIP transport protein (CPTP) remains a plausible regulatory mechanism between Golgi-CIP blocking migration and PM-CIP enhancing migration or by limiting CIP release for paracrine effects (59, 60). CERK regulation and CIP anabolism are still an enigma in the field, which was mainly due to a lack of sensitive techniques to consistently measure CIP levels accurately in cells. Although this issue is now rectified, CIP biosynthesis has not been strongly revisited. Originally, due to the very low levels of CIP in the cells versus the substrate of CERK, ceramide, conversion to CIP was not considered a plausible cellular “rheostat” for reducing ceramide levels to block proapoptotic mechanisms. The discovery of the CPTP in 2013 dispelled that dogma as these studies found a high level of “flux” of ceramide through CERK in some cell types, which was rapidly transported from the Golgi to other cellular organelles and catabolized (59). In this study, no increases in ceramides in the time frame (60 min) that CIP increases by ~2-fold was observed. Inhibition of CERK caused a marked trend in the increase of ceramide levels after mechanical trauma to cells in culture, but these differences were not significant suggesting either CERK activation or CPTP inhibition/downregulation is the mechanism of CIP induction. Nonetheless, the unique functions for specific CIP anabolic pathways require further study to elucidate their specific cellular roles, which may be opposing depending on the topology of the CIP production or cell type-specific. With recent advances in examining metabolic “flux” of sphingolipids via mass spectrometry, the regulatory mechanisms for CIP biosynthesis can be explored in the future in detail.

One of the more important outcomes of this study is the demonstration of rapid acute wound closure from CIP inhibition in vivo in a postwounding manner. Thus, topical treatment of wounds with a CERK inhibitor could be effective in enhancing wound healing and possibly even incorporated into antibiotic ointments in future studies. One of the unique strengths of SYR382141 is its ability to significantly reduce CIP levels in vivo. Additionally, CERK inhibiting drugs may also

be adaptable to chronic wounds, which fail to resolve and are “stalled” in the inflammatory stage possibly due to continued CIP production, high PGE₂ (61), and elevated neutrophil activity (62). Indeed, the main component of the venom of the Brown Recluse spider (63) is sphingomyelinase D (SMase D), which hydrolyzes sphingomyelin to CIP. The dermal necrosis/ulceration induced by SMase D is well documented in patients bitten by the Brown Recluse spider (64), which presents as ulcerative wound similar in many aspects to a pressure ulcer. Thus, the chronic synthesis of CIP would be a plausible driver of “stalled” wound healing. CERK inhibitors may have the ability to suppress the synthesis of CIP as well as PGE₂ (65), enhance 5-HETE and 5-oxo-ETE production, and induce fibroblast activation, thus promoting wound healing of stall wounds linked to neutrophilia and a chronic inflammatory stage. On the other hand, some pathogenic bacteria also have SMase D (66, 67), which may stall wound healing independent of CERK, and thus, a combination therapy of 5-oxo-ETE and CERK inhibitors may provide more benefit in a clinical setting where the wound microbiome is also a major factor in wound healing outcomes. Lastly, a better mechanistic understanding of the CERK/5-oxo-ETE interplay could be valuable for treating other diseases highly correlated to these lipid biomarkers such as preeclampsia (68, 69) and type I diabetes (70, 71).

In conclusion, this study demonstrates that enhanced wound healing and maturation is induced by blocking CERK-derived CIP, which is a negative regulator of fibroblast function and the 5-HETE/5-oxo-ETE/OXER1 axis. Our findings show the importance of sphingolipids and resulting eicosanoids in the wound healing process and provide the groundwork for foundational preclinical studies to move forward for future clinical therapeutic development of CERK inhibiting drugs that accelerate the healing rate and closure of wounds, especially for postinjury treatment.

Data availability

All data are contained within the manuscript. 

Supplemental data

This article contains [supplemental data](#) (72–80).

Acknowledgments

We would like to thank the Neuroscience Drug Discovery Unit, Takeda California, San Diego, CA, for their provision of the new ceramide kinase inhibitor, SYR382141, to test in our mouse models of wound healing.


Author contributions

K. D. M., D. J. S., H. P. M., H.-J. H., J. S., M. K., R. F. D., and C. E. C. conceptualization; H. P. M., H.-J. H., J. S., M. K., R. F. D., and C. E. C. methodology; A. N. A., H. P. M., M. K., and C. E. C. validation; K. D. M., D. J. S., H. P. M., A. N. A., and M. K. formal analysis; K. D. M., D. J. S., H.-J. H., and M. K. investigation; H.-J. H. and J. S. resources; K. D. M., D. J. S., and A. N. A. data

curation; K. D. M. and D. J. S. writing - original draft; R. F. D. and C. E. C. writing - review & editing; M. K., R. F. D., and C. E. C. supervision, C. E. C. project administration; J. S. and C. E. C. funding acquisition.

Author ORCIDs

Kenneth D. Maus  <https://orcid.org/0000-0002-2868-2934>

Henry Patrick MacKnight  <https://orcid.org/0000-0003-3232-6155>

Minjung Kim  <https://orcid.org/0000-0002-5682-6640>

Charles E. Chalfant  <https://orcid.org/0000-0002-5844-5235>

Funding and additional information

This work was supported by research grants from Takeda Corporation (C. E. C.); the Veteran’s Administration (VA Merit Review, I BX001792) (C. E. C.); and a Research Career Scientist Award, IK6BX004603 (C. E. C.); the National Institutes of Health via R01s AII39072 (C. E. C.), GM137578 (C. E. C.), DK126444 (C. E. C.), and GM137394 (C. E. C.). The CERK knockout mouse was created using funds from the Paul M. Corman, M. D. Endowed Chair in Cancer Research held by CEC when located at Virginia Commonwealth University, Richmond, VA. The contents of this manuscript do not represent the views of the Department of Veterans Affairs or the United States Government. The content is solely the responsibility of the authors and does not necessarily represent the official views of the National Institutes of Health.

Conflict of interest

The authors declare that they have no conflicts of interest with the contents of this article.

Abbreviations

5-oxo-ETE, 5-Oxo-eicosatetraenoic acid; AA, arachidonic acid; CIP, ceramide-1-phosphate; CERK, ceramide kinase; CERK-KO, CERK-knockout; cPLA₂α, cytosolic phospholipase A₂ alpha; CPTP, CIP transport protein; COX, cyclooxygenase; EGF, epidermal growth factor; FAP, fibroblast activation protein; FLAP, 5-lipoxygenase-activating protein; HUVEC, human umbilical vein endothelial cell; LOX, lipoxygenase; NVP-231, N-[2-(Benzoylamino)-6-benzothiazolyl]tricyclo[3.3.1.1^{3,7}]decane-1-carboxamide; OXER1, oxoeicosanoid receptor 1; pDFs, primary dermal fibroblasts; PGE₂, prostaglandin E₂; PM, plasma membrane.

Manuscript received November 9, 2021, and in revised form February 18, 2022. Published, JLR Papers in Press, February 24, 2022, <https://doi.org/10.1016/j.jlr.2022.100187>

REFERENCES

1. Clark, R. A. F. (1988) Wound repair. In *The Molecular and Cellular Biology of Wound Repair*. R. A. F. Clark, editor. Springer, Boston, MA, 3–50
2. Versteeg, H. H., Heemskerk, J. W. M., Levi, M., and Reitsma, P. H. (2013) New fundamentals in hemostasis. *Physiol. Rev.* **93**, 327–358
3. Diegelmann, R. F., and Evans, M. C. (2004) Wound healing: an overview of acute, fibrotic and delayed healing. *Front. Biosci.* **9**, 283–289
4. Koh, T. J., and DiPietro, L. A. (2011) Inflammation and wound healing: the role of the macrophage. *Expert Rev. Mol. Med.* **13**, e23

5. Broughton, G., Janis, J. E., and Attinger, C. E. (2006) Wound healing: an overview. *Plast. Reconstr. Surg.* **117**, 1eS–32eS
6. Ireton, J. E., Unger, J. G., and Rohrich, R. J. (2013) The role of wound healing and its everyday application in plastic surgery: a practical perspective and systematic review. *Plast. Reconstr. Surg. Glob. Open.* **1**, e10–e19
7. Stacey, M. (2011) Chronic venous insufficiency and leg ulceration: Principles and vascular biology. In *Mechanisms of Vascular Disease: A Reference Book for Vascular Specialists [Internet]*. R. Fitzridge and M. Thompson, editors. University of Adelaide Press, Adelaide, Australia, 25
8. Berwick, M. L., Dudley, B. A., Maus, K., and Chalfant, C. E. (2019) The role of ceramide 1-phosphate in inflammation, cellular proliferation, and wound healing. In J. Stiban, editor, *Bioactive Ceramides in Health and Disease. Advances in Experimental Medicine and Biology* (Vol. 1159), Springer, Cham, 65–77
9. Dhall, S., Wijesinghe, D. S., Karim, Z. A., Castro, A., Vemana, H. P., Khasawneh, F. T., Chalfant, C. E., and Martins-Green, M. (2015) Arachidonic acid-derived signaling lipids and functions in impaired healing. *Wound Repair Regen.* **23**, 644–656
10. Romana-Souza, B., Santos, J. S., Bandeira, L. G., and Monte-Alto-Costa, A. (2016) Selective inhibition of COX-2 improves cutaneous wound healing of pressure ulcers in mice through reduction of iNOS expression. *Life Sci.* **153**, 82–92
11. White, E. S., Atrasz, R. G., Dickie, E. G., Aronoff, D. M., Stambolic, V., Mak, T. W., Moore, B. B., and Peters-Golden, M. (2005) Prostaglandin E₂ inhibits fibroblast migration by E-prostanoid 2 receptor-mediated increase in PTEN activity. *Am. J. Respir. Cell Mol. Biol.* **32**, 135–141
12. Ruzicka, T. (1990) Eicosanoids and the Skin 1st Ed. CRC Press, Boca Raton, FL
13. Rieger, G. M., Hein, R., Adelman-Grill, B. C., Ruzicka, T., and Krieg, T. (1990) Influence of eicosanoids on fibroblast chemotaxis and protein synthesis in vitro. *J. Dermatol. Sci.* **1**, 347–354
14. Stephenson, D. J., MacKnight, H. P., Hoeflerlin, L. A., Park, M. A., Allegood, J. C., Cardona, C. L., and Chalfant, C. E. (2019) A rapid and adaptable lipidomics method for quantitative UPLC-mass spectrometric analysis of phosphatidylethanolamine and phosphatidylcholine: in vitro, and in cells. *Anal. Methods.* **11**, 1765–1776
15. Clark, J. D., Schievella, A. R., Nalefski, E. A., and Lin, L. L. (1995) Cytosolic phospholipase A₂. *J. Lipid Mediat. Cell Signal.* **12**, 83–117
16. Pettus, B. J., Bielawska, A., Subramanian, P., Wijesinghe, D. S., Maceyka, M., Leslie, C. C., Evans, J. H., Freiberg, J., Roddy, P., Hannun, Y. A., and Chalfant, C. E. (2004) Ceramide 1-phosphate is a direct activator of cytosolic phospholipase A₂. *J. Biol. Chem.* **279**, 11320–11326
17. Pettus, B. J., Bielawska, A., Spiegel, S., Roddy, P., Hannun, Y. A., and Chalfant, C. E. (2003) Ceramide kinase mediates cytokine- and calcium ionophore-induced arachidonic acid release. *J. Biol. Chem.* **278**, 38206–38213
18. Wijesinghe, D. S., Subramanian, P., Lamour, N. F., Gentile, L. B., Granado, M. H., Bielawska, A., Szulc, Z., Gomez-Munoz, A., and Chalfant, C. E. (2009) Chain length specificity for activation of cPLA₂α by CIP: use of the dodecane delivery system to determine lipid-specific effects. *J. Lipid Res.* **50**, 1986–1995
19. Ward, K. E., Bhardwaj, N., Vora, M., Chalfant, C. E., Lu, H., and Stahelin, R. V. (2013) The molecular basis of ceramide-1-phosphate recognition by C2 domains. *J. Lipid Res.* **54**, 636–648
20. Stahelin, R. V., Subramanian, P., Vora, P., Cho, W., and Chalfant, C. E. (2007) Ceramide-1-phosphate binds group IVA cytosolic phospholipase A₂ via a novel site in the C2 domain. *J. Biol. Chem.* **282**, 20467–20474
21. Lamour, N. L., Wijesinghe, D. S., Subramanian, P., Stahelin, R. V., Bonventre, J. V., and Chalfant, C. E. (2009) Ceramide-1-phosphate is required for the translocation of group IVA cytosolic phospholipase A₂ and prostaglandin synthesis. *J. Biol. Chem.* **284**, 26897–26907
22. Wijesinghe, D. S., Brentnall, M., Mietla, J. A., Hoeflerlin, L. A., Diegelmann, R. F., Boise, L. H., and Chalfant, C. E. (2014) Ceramide kinase is required for a normal eicosanoid response and the subsequent orderly migration of fibroblasts. *J. Lipid Res.* **55**, 1298–1309
23. MacKnight, H. P., Stephenson, D. J., Hoeflerlin, L. A., Benusa, S. D., DeLigio, J. T., Maus, K. D., Ali, A. N., Wayne, J. S., Park, M. A., Hinchcliffe, E. H., Brown, R. E., Ryan, J. J., Diegelmann, R. F., and Chalfant, C. E. (2019) The interaction of ceramide 1-phosphate with group IVA cytosolic phospholipase A₂ coordinates acute wound healing and repair. *Sci. Signal.* **12**, eaav5918
24. Paronetto, M. P., Achsel, T., Massiello, A., Chalfant, C. E., and Sette, C. (2007) The RNA-binding protein Sam68 modulates the alternative splicing of Bcl-x. *J. Cell Biol.* **176**, 929–939
25. Gowda, S. G. B., Gowda, D., Kain, V., Chiba, H., Hui, S-P., Chalfant, C. E., Parcha, V., Arora, P., and Halade, G. V. (2021) Sphingosine-1-phosphate interactions in the spleen and heart reflect extent of cardiac repair in mice and failing human hearts. *Am. J. Physiol. Heart Circ. Physiol.* **321**, H599–H611
26. DeLigio, J. T., Lin, G., Chalfant, C. E., and Park, M. A. (2017) Splice variants of cytosolic polyadenylation element-binding protein 2 (CPEB2) differentially regulate pathways linked to cancer metastasis. *RNA.* **292**, P17909–P17918
27. Caslin, H. L., Abeyayehu, D., Qayum, A. A., Haque, T. T., Taruselli, M. T., Paez, P. A., Pondicherry, N., Barnstein, B. O., Hoeflerlin, L. A., Chalfant, C. E., and Ryan, J. J. (2019) Lactic acid inhibits lipopolysaccharide-induced mast cell function by limiting glycolysis and ATP availability. *J. Immunol.* **203**, 453–464
28. Chalfant, C. E., Rathman, K., Pinkerman, R. L., Wood, R. E., Obeid, L. M., Ogretmen, B., and Hannun, Y. A. (2002) De novo ceramide regulates the alternative splicing of caspase 9 and Bcl-x in A549 lung adenocarcinoma cells. Dependence on protein phosphatase-1. *J. Biol. Chem.* **277**, 12587–12595
29. Hill, K. S., Roberts, E. R., Wang, X., Marin, E., Park, T. D., Son, S., Ren, Y., Fang, B., Yoder, S., Kim, S., Kim, S., Wan, L., Sarnaik, A. A., Koomen, J. M., Messina, J. L., Teer, J. K., et al. (2019) *PTPN11* plays oncogenic roles and is a therapeutic target for *BRAF* wild-type melanomas. *Mol. Cancer Res.* **17**, 583–593
30. Seluanov, A., Vaidya, A., and Gorbunova, V. (2010) Establishing primary adult fibroblast cultures from rodents. *J. Vis. Exp.* **44**, 2033
31. Hoeflerlin, L. A., Huynh, Q. K., Mietla, J. A., Sell, S. A., Tucker, J., Chalfant, C. E., and Wijesinghe, D. S. (2015) The lipid portion of activated platelet-rich plasma significantly contributes to its wound healing properties. *Adv. Wound Care.* **4**, 100–109
32. Hankins, J. L., Ward, K. E., Linton, S. S., Barth, B. M., Stahelin, R. V., Fox, T. E., and Kester, M. (2013) Ceramide 1-phosphate mediates endothelial cell invasion via the annexin a2-p11 heterotetrameric protein complex. *J. Biol. Chem.* **288**, 19726–19738
33. Nelson, A. J., Stephenson, D. J., Cardona, C. L., Lei, X., Almutairi, A., White, T. D., Tusing, Y. G., Park, M. A., Barbour, S. E., Chalfant, C. E., and Ramanadham, S. (2020) Macrophage polarization is linked to Ca²⁺-independent phospholipase A₂β-derived lipids and cross-cell signaling in mice. *J. Lipid Res.* **61**, 143–148
34. Hirano, Y., Gao, Y. G., Stephenson, D. J., Vu, N. T., Malinina, L., Simanshu, D. K., Chalfant, C. E., Patel, D. J., and Brown, R. E. (2019) Structural basis of phosphatidylcholine recognition by the c2-domain of cytosolic phospholipase a2α. *Elife.* **8**, e44760
35. Mishra, S. E., Stephenson, D. J., Chalfant, C. E., and Brown, R. E. (2019) Upregulation of human glycolipid transfer protein (GLTP) induces necroptosis in colon carcinoma cells. *Biochim. Biophys. Acta Mol. Cell Biol. Lipids.* **1864**, 158–167
36. Mitra, P., Maceyka, M., Payne, S. G., Lamour, N., Milstien, S., Chalfant, C. E., and Spiegel, S. (2007) Ceramide kinase regulates growth and survival of A549 human lung adenocarcinoma cells. *FEBS Lett.* **581**, 735–740
37. Chalfant, C. E., Ogretmen, B., Galadari, S., Kroesen, B.-J., Pettus, B. J., and Hannun, Y. A. (2001) FAS activation induces dephosphorylation of SR proteins. *J. Biol. Chem.* **276**, 44848–44855
38. Wijesinghe, D. S., and Chalfant, C. E. (2013) Systems-level lipid analysis methodologies for qualitative and quantitative investigation of lipid signaling events during wound healing. *Adv. Wound Care.* **2**, 538–548
39. Wijesinghe, D. S., Massiello, A., Subramanian, P., Szulc, Z., Bielawska, A., and Chalfant, C. E. (2005) Substrate specificity of human ceramide kinase. *J. Lipid Res.* **46**, P2706–P2716
40. Lamour, N. F., and Chalfant, C. E. (2008) Ceramide kinase and the ceramide-1-phosphate/cPLA₂α interaction as a therapeutic target. *Curr. Drug Targets.* **9**, 674–682
41. Van Overloop, H., Gijsbers, S., and Van Veldhoven, P. P. (2006) Further characterization of mammalian ceramide kinase: substrate delivery and (stereo)specificity, tissue distribution, and subcellular localization studies. *J. Lipid Res.* **47**, 268–283
42. Don, A. S., and Rosen, H. (2008) A fluorescent plate reader assay for ceramide kinase. *Anal. Biochem.* **375**, 265–271

43. Graf, C., Rovina, P., and Bornancin, F. (2009) A secondary assay for ceramide kinase inhibitors based on cell growth inhibition by short-chain ceramides. *Anal. Biochem.* **384**, 166–169
44. Pettus, B. J., Bielawski, J., Porcelli, A. M., Reames, D. L., Johnson, K. R., Morrow, J., Chalfant, C. E., Obeid, L. M., and Hannun, Y. A. (2003) The sphingosine kinase 1/sphingosine-1-phosphate pathway mediates COX-2 induction and PGE2 production in response to TNF- α . *FASEB J.* **17**, 1411–1421
45. Slon-Usakiewicz, J. J., Dai, J.-R., Ng, W., Foster, J. E., Deretey, E., Toledo-Sherman, L., Redden, P. R., Pasternak, A., and Reid, N. (2005) Global kinase screening. Applications of frontal affinity chromatography coupled to mass spectrometry in drug discovery. *Anal. Chem.* **77**, 1268–1274
46. Konya, V., Bfättermann, S., Jandl, K., Platzer, W., Ottersbach, P. A., Marsche, G., Gütschow, M., Kostenis, E., and Heinemann, A. (2014) A biased non-G α_i OXE-R antagonist demonstrates that G α_i protein subunit is not directly involved in neutrophil, eosinophil, and monocyte activation by 5-oxo-ETE. *J. Immunol.* **192**, 4774–4782
47. Bionda, C., Portoukalian, J., Schmitt, D., Rodriguez-Lafrasse, C., and Ardail, D. (2004) Subcellular compartmentalization of ceramide metabolism: MAM (mitochondria-associated membrane) and/or mitochondria? *Biochem. J.* **382**, 527–533
48. Lai, Q., Yuan, G., Shen, L., Zhang, L., Fu, F., Liu, Z., Zhang, Y., Kou, J., Liu, S., Yu, B., and Li, F. (2021) Oxoeicosanoid receptor inhibition alleviates acute myocardial infarction through activation of BCAT1. *Basic Res. Cardiol.* **116**, 3
49. Cooke, M., Di Cónsoli, H., Maloberti, P., and Maciel, F. C. (2013) Expression and function of OXE receptor, an eicosanoid receptor, in steroidogenic cells. *Mol. Cell. Endocrinol.* **371**, 71–78
50. Feingold, K. R., Moser, A., Shigenaga, J. K., and Grunfeld, C. (2014) Inflammation stimulates niacin receptor (GPR109A/HCA2) expression in adipose tissue and macrophages. *J. Lipid Res.* **55**, 2501–2508
51. Stephenson, D. J., Hoferlin, L. A., and Chalfant, C. E. (2017) Lipidomics in translational research and the clinical significance of lipid-based biomarkers. *Transl. Res.* **189**, 13–29
52. Ohto, T., Uozumi, N., Hirabayashi, T., and Shimizu, T. (2005) Identification of novel cytosolic phospholipase A₂s, murine cPLA₂ δ , ϵ , and ζ , which form a gene cluster with cPLA₂ β . *J. Biol. Chem.* **280**, 24576–24583
53. Ghomashchi, F., Naika, G. S., Bollinger, J. G., Aloulou, A., Lehr, M., Leslie, C. C., and Gelb, M. H. (2015) Interfacial kinetic and binding properties of mammalian group IVB phospholipase A₂ (cPLA₂ β) and comparison with the other cPLA₂ isoforms. *J. Biol. Chem.* **285**, 36100–36111
54. Granado, M. H., Gangoiti, P., Ouro, A., Arana, L., González, M., Trueba, M., and Gómez-Muñoz, A. (2009) Ceramide 1-phosphate (C1P) promotes cell migration: involvement of a specific C1P receptor. *Cell Signal.* **21**, 405–412
55. Rivera, I. G., Ordoñez, M., Presa, N., Gangoiti, P., Gomez-Larauri, A., Trueba, M., Fox, T., Kester, M., and Gomez-Muñoz, A. (2016) Ceramide 1-phosphate regulates cell migration and invasion of human pancreatic cancer cells. *Biochem. Pharmacol.* **102**, 107–119
56. Katz, S., Ernst, O., Avni, D., Athamna, M., Philosoph, A., Arana, L., Ouro, A., Hoferlin, L. A., Meijler, M. M., Chalfant, C. E., Gomez-Munoz, A., and Zor, T. (2016) Exogenous ceramide-1-phosphate (C1P) and phospho-ceramide analogue-1 (PCERA-1) regulate key macrophage activities via distinct receptors. *Immunol. Lett.* **169**, 73–81
57. Mishra, S. K., Gao, Y.-G., Zou, X., Stephenson, D. J., Malinina, L., Hinchcliffe, E. H., Chalfant, C. E., and Brown, R. E. (2020) Emerging roles for human glycolipid transfer protein superfamily members in the regulation of autophagy, inflammation, and cell death. *Prog. Lipid Res.* **78**, 101031
58. Lamour, N. F., Stahelin, R. V., Wijesinghe, D. S., Maceyka, M., Wang, E., Allegood, J. C., Merrill, A. H., Jr., Cho, W., and Chalfant, C. E. (2007) Ceramide kinase uses ceramide provided by ceramide transport protein: localization to organelles of eicosanoid synthesis. *J. Lipid Res.* **48**, 1293–1304
59. Simanshu, D. K., Kamlekar, R. K., Wijesinghe, D. S., Zou, X., Zhai, X., Mishra, S. K., Molotkovsky, J. G., Malinina, L., Hinchcliffe, E. H., Chalfant, C. E., Brown, R. E., and Patel, D. J. (2013) Non-vesicular trafficking by a ceramide-1-phosphate transfer protein regulates eicosanoids. *Nature.* **500**, 463–467
60. Mishra, S. K., Gao, Y.-G., Deng, Y., Chalfant, C. E., Hinchcliffe, E. H., and Brown, R. E. (2018) CPTP: a sphingolipid transfer protein that regulates autophagy and inflammasome activation. *Autophagy.* **14**, 862–879
61. Parekh, A., Sandulache, V. C., Singh, T., Cetin, S., Sacks, M. S., Dohar, J. E., and Hebda, P. A. (2009) Prostaglandin E₂ differentially regulates contraction and structural reorganization of anchored collagen gels by human adult and fetal dermal fibroblasts. *Wound Repair Regen.* **17**, 88–98
62. Kim, M.-H., Liu, W., Borjesson, D. L., Curry, F.-R. E., Miller, L. S., Cheung, A. L., Liu, F.-T., Isseroff, R. R., and Simon, S. I. (2008) Dynamics of neutrophil infiltration during cutaneous wound healing and infection using fluorescence imaging. *J. Invest. Dermatol.* **128**, 1812–1820
63. Truett III, A. P., and King, L. E., Jr. (1993) Sphingomyelinase D: a pathogenic agent produced by bacteria and arthropods. *Adv. Lipid Res.* **26**, 275–291
64. Rees, R. S., Nanney, L. B., Yates, R. A., and King, L. E., Jr. (1984) Interaction of brown recluse spider venom on cell membranes: the inciting mechanism? *J. Invest. Dermatol.* **83**, 270–275
65. Pettus, B. J., Kitatani, K., Chalfant, C. E., Taha, T. A., Kawamori, T., Bielawski, J., Obeid, L. M., and Hannun, Y. A. (2005) The co-ordination of prostaglandin E₂ production by sphingosine-1-phosphate and ceramide-1-phosphate. *Mol. Pharmacol.* **68**, 330–335
66. Mariotti, R. B., Chaves-Moreira, D., Vuitika, L., Caruso, Í. P., Coronado, M. A., Azevedo, V. A., Murakami, M. T., Veiga, S. S., and Arni, R. K. (2017) Bacterial and arachnid sphingomyelinases D: comparison of biophysical and pathological activities. *J. Cell. Biochem.* **118**, 2053–2063
67. Cockburn, C. L., Green, R. S., Damle, S. R., Martin, R. K., Ghahrai, N. N., Colonne, P. M., Fullerton, M. S., Conrad, D. H., Chalfant, C. E., Voth, D. E., Rucks, E. A., Gilk, S. D., and Carlyon, J. A. (2019) Functional inhibition of acid sphingomyelinase disrupts infection by intracellular bacterial pathogens. *Life Sci. Alliance.* **2**, e201800292
68. Walsh, S. W., Reep, D. T., Alam, S. M. K., Washington, S. L., Al Dulaimi, M., Lee, S. M., Springel, E. H., Strauss III, J. F., Stephenson, D. J., and Chalfant, C. E. (2020) Placental production of eicosanoids and sphingolipids in women who developed pre-eclampsia on low-dose aspirin. *Reprod. Sci.* **27**, 2158–2169
69. Amraoui, F., Hassani Lahsinoui, H., Spijkers, L. J. A., Vogt, L., Peters, S. L. M., Wijesinghe, D. S., Warncke, U. O., Chalfant, C. E., Ris-Stalpers, C., van den Born, B.-J. H., and Afink, G. B. (2020) Plasma ceramide is increased and associated with proteinuria in women with pre-eclampsia and HELLP syndrome. *Pregnancy Hypertens.* **19**, 100–105
70. Nelson, A. J., Stephenson, D. J., Bone, R. N., Cardona, C. L., Park, M. A., Tusing, Y. G., Lei, X., Kokotos, G., Graves, C. L., Mathews, C. E., Kramer, J., Hessner, M. J., Chalfant, C. E., and Ramanadham, S. (2020) Lipid mediators and biomarkers associated with type 1 diabetes development. *JCI Insight.* **5**, e138034
71. Priyadarsini, S., McKay, T. B., Sarker-Nag, A., Allegood, J., Chalfant, C. E., Ma, J.-X., and Karamichos, D. (2016) Complete metabolome and lipidome analysis reveals novel biomarkers in the human diabetic corneal stroma. *Exp. Eye Res.* **153**, 90–100
72. Van Overloop, H., Van der Hoeven, G., and Van Veldhoven, P. P. (2012) A nonradioactive fluorimetric SPE-based ceramide kinase assay using NBD-C₆-ceramide. *J. Lipids.* **2012**, 404513
73. Munagala, N., Nguyen, S., Lam, W., Lee, J., Joly, A., McMillan, K., and Zhang, W. (2007) Identification of small molecule ceramide kinase inhibitors using a homogeneous chemiluminescence high throughput assay. *Assay Drug Dev. Technol.* **5**, 65–73
74. Graf, C., Klumpp, M., Habig, M., Rovina, P., Billich, A., Baumrucker, T., Oberhauser, B., and Bornancin, F. (2008) Targeting ceramide metabolism with a potent and specific ceramide kinase inhibitor. *Mol. Pharmacol.* **74**, 925–932
75. Wells, C. I., Al-Ali, H., Andrews, D. M., Asquith, C. R. M., Axtman, A. D., Dikic, I., Ebner, D., Ettmayer, P., Fischer, C., Frederiksen, M., Futrell, R. E., Gray, N. S., Hatch, S. B., Knapp, S., Lücking, U., et al. (2021) The kinase chemogenomic set (KCGS): an open science resource for kinase vulnerability identification. *Int. J. Mol. Sci.* **22**, 566
76. Vu, N. T., Park, M. A., Schultz, M. D., Gamze, B. B., Ladd, A. C., and Chalfant, C. E. (2016) Caspase-9b interacts directly with cIAP1 to drive agonist-independent activation of NF- κ B and lung tumorigenesis. *Cancer Res.* **76**, 2977–2989

77. Goehle, R. W., Shultz, J. C., Murudkar, C., Usanovic, S., Lamour, N. F., Massey, D. H., Zhang, L., Camidge, D. R., Shay, J. W., Minna, J. D., and Chalfant, C. E. (2010) hnRNP L regulates the tumorigenic capacity of lung cancer xenografts in mice via caspase-9 pre-mRNA processing. *J. Clin. Invest.* **120**, 3923–3939
78. Shultz, J. C., Goehle, R. W., Wijesinghe, D. S., Murudkar, C., Hawkins, A. J., Shay, J. W., Minna, J. D., and Chalfant, C. E. (2010) Alternative splicing of caspase 9 is modulated by the phosphoinositide 3-kinase/Akt pathway via phosphorylation of SRp30a. *Cancer Res.* **70**, 9185–9196
79. Shultz, J. C., Goehle, R. W., Murudkar, C. S., Wijesinghe, D. S., Mayton, E. K., Massiello, A., Hawkins, A. J., Mukerjee, P., Pinkerman, R. L., Park, M. A., and Chalfant, C. E. (2011) SRSF1 regulates the alternative splicing of caspase 9 via a novel intronic splicing enhancer affecting the chemotherapeutic sensitivity of non-small cell lung cancer cells. *Mol. Cancer Res.* **9**, 889–900
80. Vu, N., Park, M., Shultz, J., Goehle, R., Hoeflerlin, L. A., Shultz, M., Smith, S., Lynch, K., and Chalfant, C. (2013) hnRNP U enhances caspase-9 splicing and is modulated by AKT-dependent phosphorylation of hnRNP L. *J. Biol. Chem.* **288**, 8575–8584